Motion-aware Self-supervised Video Representation Learning via Foreground-background Merging

Shuangrui Ding[1*], Maomao Li[2], Tianyu Yang[2], Rui Qian[3],
Haohang Xu[1], Qingyi Chen[4], Jue Wang[2]

[1] Shanghai Jiao Tong University, [2] Tencent AI Lab, [3] The Chinese University of Hong Kong, [4] University of Michigan
{dsr1212, xuhaohang}@sjtu.edu.cn, tianyu-yang@outlook.com, qr021@ie.cuhk.edu.hk, {limaomao07, arphid}@gmail.com

Abstract

In light of the success of contrastive learning in the image domain, current self-supervised video representation learning methods usually employ contrastive loss to facilitate video representation learning. When naively pulling two augmented views of a video closer, the model however tends to learn the common static background as a shortcut but fails to capture the motion information, a phenomenon dubbed as background bias. This bias makes the model suffer from weak generalization ability, leading to worse performance on downstream tasks such as action recognition. To alleviate such bias, we propose **F**oreground-b**a**ckground **Me**rging (FAME) to deliberately compose the foreground region of the selected video onto the background of others. Specifically, without any off-the-shelf detector, we extract the foreground and background regions via the frame difference and color statistics, and shuffle the background regions among the videos. By leveraging the semantic consistency between the original clips and the fused ones, the model focuses more on the foreground motion pattern and is thus more robust to the background context. Extensive experiments demonstrate that FAME can significantly boost the performance in different downstream tasks with various backbones. When integrated with MoCo, FAME reaches 84.8% and 53.5% accuracy on UCF101 and HMDB51, respectively, achieving the state-of-the-art performance.

1 Introduction

The recent development of deep learning has promoted a series of applications in videos (Wang et al. 2016; Tran et al. 2018; Feichtenhofer et al. 2019). Meanwhile, practitioners have developed various large-scale benchmarks (Abu-El-Haija et al. 2016; Carreira and Zisserman 2017; Goyal et al. 2017) accessible to the traditional fully-supervised learning methods and have greatly facilitated video-related research. Nevertheless, the high cost of manual annotation involved in fully-supervised methods excludes the potential utilization of millions of uncurated videos on the Internet. Therefore, video representation learning in an unsupervised manner is of great significance and emerges as a general trend.

Recently, unsupervised learning in images (Oord, Li, and Vinyals 2018; Wu et al. 2018; Tian, Krishnan, and Isola 2019) has achieved competitive performances compared to

---
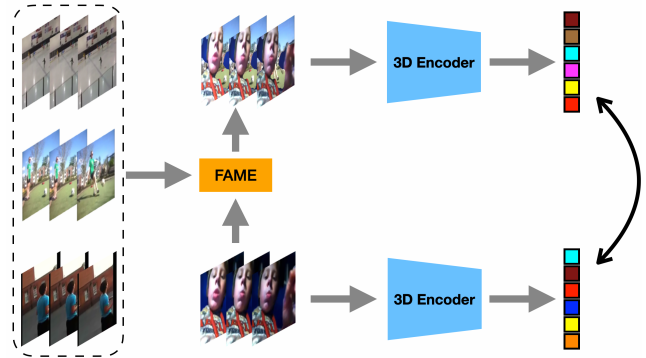*Work performed while Shuangrui was at Tencent AI Lab.

Figure 1: The contrastive learning framework with the FAME method. We first randomly sample two clips from a video and use FAME to generate new clips by composing the original foreground onto various backgrounds from other videos. We then feed the augmented clips into the existing contrastive learning framework and perform self-supervised pretraining.

their supervised counterparts, especially with the contrastive self-supervised learning formulation (He et al. 2020; Chen et al. 2020a). Inspired by these successes, various attempts have also been made in self-supervised video representation learning (Qian et al. 2020; Han, Xie, and Zisserman 2020b). However, videos are distinct from images due to the extra dimension of temporal dynamics. Unfortunately, the existing video benchmarks present severe static bias (He et al. 2016; Li, Li, and Vasconcelos 2018; Choi et al. 2019), which induces the model to focus on the static and straightforward cues like background context instead of the motion patterns that are intrinsically more informative. Therefore, when generalizing to novel benchmarks, the scene-biased model struggles to recognize some unseen action classes in the seen background. For instance, the action of "yoga" in the pretrain dataset often happens in the gym, so the pretrained model inclines to bind the yoga action to the gym scene blindly but fails to understand the essence of the "yoga" action. On the other hand, when the unseen action class of "push-up" also occurs in the gym in the downstream dataset, the pretrained model has difficulty adapting to a new action that takes place in the same scene. In short,

previous models tend to focus on background context but neglect moving foreground. This phenomenon is more severe in self-supervised learning since the model is trained without semantic supervision, i.e., action labels.

Driven by the motivation of mitigating the background bias in the self-supervised learning framework, BE (Wang et al. 2021b) proposes a simple method of adding a specific static frame on all other frames in the video. By doing so, their method can reduce the learning emphasis on the background to some extent and make the model generalize better. However, this simple operation is relatively coarse and does not take good care of the foreground region. Although adding one static frame distracts the background pixels as expected, it damages the appearance and the motion patterns of the foreground objects at the same time, leading to impaired temporal modeling and motion understanding. To ameliorate the aforementioned limitation and help the model better grasp the foreground action, we present a new augmentation technique named **F**oreground-**b**ackground **Me**rging (FAME). Particularly, we separate each video's foreground and background regions, and then merge foreground areas with random backgrounds. In the separation step, we first circle out the edge region of the moving object as the seed region via frame difference. Then, we use color statistics to extrapolate the entire foreground area from the seed region. This efficient foreground discovery method extracts most areas of dynamic on which we expect the model to put the emphasis. Next, in the merging step, we fuse the extracted foreground regions of each video with random backgrounds from other videos to form action samples. This merging step aims to reduce the influence of the original background by introducing diverse backgrounds. After that, we force the model to learn the consistent representation between original clips and distracting clips. The training pipeline is shown in Figure 1. In this way, the model is asked to prioritize the motion patterns and alleviate the background bias in the self-supervised learning framework.

We evaluate FAME on two action recognition benchmarks. The superior experimental performance verifies that FAME enables self-supervised video representation learning to generalize better and distill the motion-aware representations. In short, we summarize our contributions as follows:

- We propose a simple yet effective augmentation method for self-supervised video representation learning. Our approach helps the model mitigate background bias in video benchmarks and learn the motion-aware representations.
- Our method enhances the MoCo framework remarkably and achieves the start-of-the-art performance on two downstream tasks, action recognition and video retrieval, on two mainstream datasets, UCF101 and HMDB51.

2 Related Work

Contrastive Visual Representation Learning. Recently, contrastive learning has greatly facilitated self-supervised visual representation learning (Wu et al. 2018; Oord, Li, and Vinyals 2018; Tian, Krishnan, and Isola 2019; Chen et al.

2020a; He et al. 2020). It performs instance discrimination in a fully self-supervised manner to pull the representations of the same instance close and push those of different instances far away. Following this idea, Wu et al. (2018) proposes to formulates the instance discrimination as a non-parametric classification problem. Oord, Li, and Vinyals (2018) mathematically proves that we could estimate mutual information with InfoNCE loss (Gutmann and Hyvärinen 2010), which can be easily used for optimization. Later, He et al. (2020) proposes MoCo to make use of key representations calculated in previous iterations as negative samples to facilitate contrastive learning. Also, SimCLR (Chen et al. 2020a) proposes to employ a large batch size instead of the memory bank to expand the negative pool for more robust visual representation. Considering that SimCLR requires tremendous computational resources, we adopt the MoCo framework as a strong baseline for self-supervised pretraining in our work.

Self-supervised Video Representation Learning. In video representation learning, there has been a line of works that employ diverse pretext tasks for self-supervised representation learning (Misra, Zitnick, and Hebert 2016; Lee et al. 2017; Xu et al. 2019). The most prevalent approaches include temporal order prediction (Misra, Zitnick, and Hebert 2016), video colorization (Vondrick et al. 2018), spatio-temporal puzzling (Kim, Cho, and Kweon 2019) and speed prediction (Benaim et al. 2020). These methods generally employ manually designed tasks to seek the spatio-temporal cues in video data, but the performance is limited. Then, for further improvement, some works apply contrastive learning formulation into video representation learning (Gordon et al. 2020; Qian et al. 2020). Han et al. use InfoNCE loss to guide dense predictive coding in videos (Han, Xie, and Zisserman 2019, 2020a). Asano, Rupprecht, and Vedaldi (2019); Han, Xie, and Zisserman (2020b) propose to leverage the consistency between different modalities to enhance video representation. However, the video representations learned from these methods are mostly dominated by the background instead of the dynamic motions (Wang et al. 2021b), which introduces strong background bias and impairs generalization ability in downstream applications. Therefore, we now propose FAME to construct positive samples with the same motions but different backgrounds for self-supervised pretraining in this work.

Video Background Bias Mitigation. How to mitigate the background bias has been a long-standing topic for action recognition. In the supervised scenario, Choi et al. (2019) use an off-the-shelf human detector to mask out the human regions and train the model in an adversarial manner. Later, to make the self-supervised video representations more robust to the background bias, a line of works employ other natural supervision (Huang et al. 2021b; Xiao, Tighe, and Modolo 2021) to guide the model to capture motion information explicitly. However, these methods require more than one backbone to pretrain multi-modality data, resulting in an undesired computational cost. To better leverage the implicit motion information in videos, DSM (Wang et al. 2021a) aims to decouple the motion and context by deliberately constructing the positive/negative samples through spatial and temporal disturbance. BE (Wang et al. 2021b) proposes to

add a static frame as background noise for static bias mitigation. But these two methods would erode the foreground moving objects, while our FAME meticulously extracts foreground regions and preserves high-quality motion patterns.

3 Approach

In this section, we introduce our Foreground-background Merging (FAME) method. In section 3.1, we first revisit the vanilla contrastive learning framework and then illustrate how our method is applied in this framework. In section 3.2, we elaborate on how to separate foreground regions using our method. To clarify the notation, we denote the video clips as $X \in R^{C \times T \times H \times W}$, where C, T, H, W are respectively the dimension of the channel, timespan, height, width.

3.1 Vanilla Contrastive Learning

The vanilla contrastive learning approach employs instance discrimination to learn the feature representation in a fully self-supervised manner (Chen et al. 2020a; He et al. 2020; Grill et al. 2020). Generally, it aims to maximize the similarity between the query sample q and its positive keys k^+, and minimize the similarity between q and negative keys k^-. We empirically use InfoNCE loss (Gutmann and Hyvärinen 2010) for optimization:

$$\mathcal{L}_{nce} = -\log \frac{\sum_{k \in \{k^+\}} \exp(\text{sim}(q,k)/\tau)}{\sum_{k \in \{k^+, k^-\}} \exp(\text{sim}(q,k)/\tau)}, \quad (1)$$

where τ is the temperature hyper-parameter controlling the concentration level of the distribution, and $\text{sim}(q,k)$ measures the cosine similarity between the latent embeddings, i.e., $\text{sim}(q,k) = q^T k/(\|q\|_2 \|k\|_2)$. In most existing works (Feichtenhofer et al. 2021), k^+ is the set of clip embeddings extracted from the same video as q, and k^- is the set of clip embeddings extracted from other videos.

However, this vanilla contrastive learning formulation in the video domain cannot fully utilize the dynamic motion information and tends to discriminate different instances according to the background cues (Wang et al. 2021b). If the model depends excessively on the background but ignores the foreground object, such a misleading focus can risk the model's generalization ability. Thus, we carefully design FAME as an augmentation technique to circumvent the negative impact of the background. We show the contrastive learning framework with FAME in Figure 1. In detail, we randomly sample two clips from different timestamps. Before applying the basic augmentation, we use our proposed FAME method to compound the foreground of one clip with the background from other videos in the same mini-batch. After that, the two clips only resemble each other in the moving foreground objects but differ in the background context. Then, we feed these two clips into the 3D encoder and treat them as the positive keys while the rest of the clips serve as negative keys. Finally, we minimize the InfoNCE loss to pretrain the 3D encoder. By constructing the positive pair with the same foreground but diverse backgrounds, we guide the model to focus on temporal dynamics and suppress the impact of the background.

3.2 Foreground-background Merging

Motivated by mitigating background bias in self-supervised video representation learning, we intend to retain the foreground regions in original videos and shuffle the background areas among various videos. To achieve this goal, we propose the Foreground-background Merging method to augment the clips with minimal computation overhead. Concretely, FAME consists of two stages, one for separation and the other for merging.

In the separation stage, we show the pipeline in Figure 2. We first differentiate adjacent frames iteratively and then sum up the magnitude of the difference along channel and timespan dimensions to generate the seed region S. We formulate $S \in \mathbb{R}^{H \times W}$ as

$$S = \frac{1}{T-1} \sum_{c=1}^{C} \sum_{t=1}^{T-1} \|X_{c,t+1} - X_{c,t}\|_1. \quad (2)$$

The intuition is that moving foreground objects tend to possess a great magnitude in terms of frame difference, while the static backgrounds are minor in this metric. In practice, we find that the large values of the seed region S usually correspond to the moving objects' edge region. To expand the edge of the foreground objects into the whole foreground, we take inspiration from the unsupervised foreground discovery (Stretcu and Leordeanu 2015) for seed propagation. Specifically, we leverage the color distributions to estimate the entire foreground. Denoting $N^{(F)}$ as the total number of pixels in the foreground region and $N_x^{(F)}$ as the number of the given color x appearing in the foreground region, the probability of a given color x appearing in the foreground region can be estimated as $P(x \mid F) = N_x^{(F)}/N^{(F)}$. Similarly, the probability of x belonging to the background region is $P(x \mid B) = N_x^{(B)}/N^{(B)}$. In practice, we sample the foreground color distribution in the top 50% of seed region S and the background color distribution in the last 10% of seed region S. Namely, in our setting, $N^{(F)} = [0.5 \times H \times W]$ and $N^{(B)} = [0.1 \times H \times W]$. Given the above two distributions for the color x and the assumption that all pixels with the same color have the same probability of being the foreground and background, we approximate the foreground likelihood for a given color x as

$$P(F \mid x) = \frac{P(x \mid F)}{P(x \mid F) + P(x \mid B)}. \quad (3)$$

Therefore, the soft segmentation mask $M \in \mathbb{R}^{H \times W}$ can be calculated based on the color of each pixel. We formulate it as $[M]_{ij} = P(F \mid x_{ij})$, where x_{ij} is the color at pixel (i,j). To better filter out the background region, we binarize the mask

$$\left[\widetilde{M}\right]_{ij} = \begin{cases} 1, \text{ if } [M]_{ij} \text{ is among Top-}[\beta HW] \text{ of } M, \\ 0, \text{ otherwise,} \end{cases} \quad (4)$$

where $\beta \in [0,1]$ is a hyper-parameter to describe the portion of the foreground. Note that the mask we generate is constant with respect of timespan T for the sake of computational efficiency. To do so, we view video clips as "image"
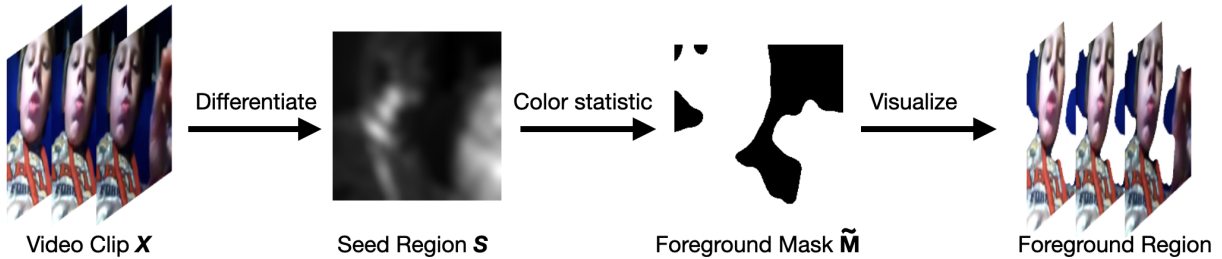
Figure 2: Separation stage of Foreground-background Merging. Given a video clip X, we can obtain seed region S by the equation (2). Then, we expand the seed region into the foreground region using color statistic assumptions.

when counting the color statistics. In other words, we reduce X over the timespan dimension, i.e., $\widetilde{X} = \sum_{t=1}^{T} X_t / T$. We have tried three variants to obtain the foreground mask $\widetilde{M}$. Experiment results in Table 6 verify that FAME works best among them. Moreover, all variants of FAME consistently enhance the representation ability greatly. It conforms to our intuition that retaining the original foregrounds and shuffling the backgrounds stimulate motion understanding. Having foreground mask $\widetilde{M}$, we then conduct the stage of merging. Denoting X, Y as foreground and background source clips, the synthetic clip $X_{\text{merge}} = X \otimes \widetilde{M} + Y \otimes (1 - \widetilde{M})$, where $\otimes$ is the element-wise multiplication. As a result, we merge the moving foreground objects with random backgrounds.

4 Experiments

In this section, we first introduce the dataset and the implementation details for our experiments. Then, we report our evaluation results on downstream tasks: action recognition, video retrieval. Next, we conduct a set of ablation studies to analyze and validate our FAME method quantitatively. Finally, we investigate and make sense of what the model learns with FAME qualitatively.

4.1 Datasets

Kinetics-400. Kinetics-400 (Carreira and Zisserman 2017) is a large-scale and high-quality dataset for action recognition, which consists of around 240K video clips with 400 human action classes. Each clip lasts about 10 seconds and is annotated with a single action class. We use the training set of Kinetics-400 to pretrain our model in a self-supervised manner.

UCF101. UCF101 (Soomro, Zamir, and Shah 2012) is a human action dataset. It contains over 13k clips covering 101 action classes. In our experiment, split 1 of UCF101 is used for pretrain and downstream tasks.

HMDB51. HMDB51 (Kuehne et al. 2011) is a human action dataset with 51 action categories and around 7,000 manually annotated clips. We also use split 1 of HMDB51 in our experiments.

4.2 Implementation Details

Self-supervised Pretraining. In the stage of self-supervised training, we apply our FAME method on MoCo framework (He et al. 2020; Chen et al. 2020b). We select two common backbone choices, R(2+1)D-18 (Tran et al. 2018) and I3D-22 (Carreira and Zisserman 2017), as the 3D encoder.

First, we randomly sample two different temporal clips in the same video as positive pair. Each clip consists of 16 frames with a temporal stride of 2. We spatially crop a random portion of clips and resize it to the size of 224×224 or 112×112. We then use FAME to distract one out of the positive pairs. Notice that the background videos are from the clips in the same mini-batch. Next, following the prior work (Feichtenhofer et al. 2021), we perform the basic augmentation containing random grayscale, color jittering, random horizontal flip, and random Gaussian blur. All these augmentations are temporally consistent. We pretrain the model for 200 epochs with a batch size of 64 on 8 Tesla V100 GPUs during the training phase. The SGD optimizer is adopted with the initial learning rate of 10^{-2} and weight decay of 10^{-4}. For the implementation of MoCo, the number of the negative queue is set to 65536 for Kinetics-400, and 2048 for UCF101, respectively. We also swap the key/queue samples so that every sample can generate the gradient for optimization. More details about implementation are in Appendix.

Action Recognition. After pretraining, we initialize the backbone with the pretrained parameters except for the last fully connected layer. There are two protocols of action recognition to validate the self-supervised representations. One is *linear probe*. The encoder is frozen, and we only train the last fully connected layer. The second one is *finetune*, where we train the whole network in a supervised fashion. During the inference phase, we take the standard evaluation protocol (Xu et al. 2019; Wang, Jiao, and Liu 2020; Pan et al. 2021). We uniformly sample ten 16-frame video clips with a temporal stride of 2 from each testing video, then center crop and resize them to 224×224 or 112×112. We average the prediction of each testing video clip and report Top-1 accuracy to measure the action recognition performance.

Video Retrieval. Without further training, we directly use the representation from the pretrained encoder for evaluation. Following Xu et al. (2019); Luo et al. (2020), we take video clips in the test set to query k nearest neighbors in the training set. In detail, we average the representation of ten uniformly sampled clips to obtain the global representation.

Method	Backbone	Pretrain Dataset	Frames	Res.	Freeze	UCF101	HMDB51
CBT (Sun et al. 2019)	S3D	Kinetics-600	16	112	✓	54.0	29.5
CCL (Kong et al. 2020)	R3D-18	Kinetics-400	16	112	✓	52.1	27.8
MemDPC (Han, Xie, and Zisserman 2020a)	R3D-34	Kinetics-400	40	224	✓	54.1	30.5
RSPNet (Chen et al. 2021)	R3D-18	Kinetics-400	16	112	✓	61.8	**42.8**
MLRep (Qian et al. 2021)	R3D-18	Kinetics-400	16	112	✓	63.2	33.4
MoCo (Chen et al. 2020b)	R(2+1)D	Kinetics-400	16	112	✓	67.4	39.8
MoCo+FAME (Ours)	R(2+1)D	Kinetics-400	16	112	✓	**72.2**(4.8↑)	42.2(2.4↑)
Shuffle (Misra, Zitnick, and Hebert 2016)	AlexNet	UCF101	3	256	✗	50.2	18.1
OPN (Lee et al. 2017)	VGG	UCF101	4	80	✗	59.8	23.8
VCP (Luo et al. 2020)	R(2+1)D	UCF101	16	112	✗	66.3	32.2
PRP (Yao et al. 2020)	R(2+1)D	UCF101	16	112	✗	72.1	35.0
IIC (Tao, Wang, and Yamasaki 2020)	C3D	UCF101	16	112	✗	72.7	36.8
TempTrans (Jenni, Meishvili, and Favaro 2020)	R(2+1)D	UCF101	16	112	✗	81.6	46.4
3DRotNet (Jing et al. 2018)	R3D-18	Kinetics-400	16	112	✗	62.9	33.7
Spatio-Temp (Wang et al. 2019)	C3D	Kinetics-400	16	112	✗	61.2	33.4
Pace Prediction (Wang, Jiao, and Liu 2020)	R(2+1)D	Kinetics-400	16	112	✗	77.1	36.6
MemDPC (Han, Xie, and Zisserman 2020a)	R3D-34	Kinetics-400	40	224	✗	78.1	41.2
SpeedNet (Benaim et al. 2020)	S3D-G	Kinetics-400	64	224	✗	81.1	48.8
VideoMoCo (Pan et al. 2021)	R(2+1)D	Kinetics-400	32	112	✗	78.7	49.2
RSPNet (Chen et al. 2021)	R(2+1)D	Kinetics-400	16	112	✗	81.1	44.6
MLRep (Qian et al. 2021)	R3D-18	Kinetics-400	16	112	✗	79.1	47.6
ASCNet (Huang et al. 2021a)	R3D-18	Kinetics-400	16	112	✗	80.5	52.3
SRTC (Zhang et al. 2021)	R(2+1)D	Kinetics-400	16	112	✗	82.0	51.2
MoCo (Chen et al. 2020b)	R(2+1)D	Kinetics-400	16	112	✗	82.9	50.7
MoCo+FAME (ours)	R(2+1)D	Kinetics-400	16	112	✗	**84.8**(1.9↑)	**53.5**(2.8↑)
DSM (Wang et al. 2021a)	I3D	Kinetics-400	16	224	✗	74.8	52.5
MoCo+BE (Wang et al. 2021b)	I3D	Kinetics-400	16	224	✗	86.8	55.4
MoCo+FAME (ours)	I3D	Kinetics-400	16	224	✗	**88.6**	**61.1**

Table 1: Comparison with the existing self-supervised video representation learning methods for action recognition on UCF101 and HMDB51. To compare fairly, we list each work's setting, including backbone architecture used, pretrain dataset and spatial-temporal resolution. Freeze (tick) indicates linear probe, and no freeze (cross) means finetune.

If the category of the testing clip appears in the k nearest neighbors, it counts as a hit. We report Top-k recall R@k for evaluation.

4.3 Evaluation on Downstream Tasks

Action Recognition. We compare our method with the existing self-supervised video representation learning approaches on action recognition. In Table 1, we report Top-1 accuracy on UCF101 and HMDB51. We do not consider the existing methods with a deeper backbone or non-single modality, e.g., optical flow, audio, and text.

Our method obtains the best result on UCF101 and a comparable result on HMDB51 in the linear probe setting. Even though MoCo (Chen et al. 2020b) serves a strong baseline and outperforms most previous methods, our FAME could still improve MoCo baseline by 4.8% and 2.4% respectively on UCF101 and HMDB51. MoCo+FAME also beats MLRep (Qian et al. 2021), which carefully designs the multi-level feature optimization and temporal modeling, by a large margin, i.e., about 9.0% gain on both UCF101 and HMDB51. The outstanding performance demonstrates that

our method can capture the moving foreground patterns and represent the temporal information.

In the finetune protocol, FAME with R(2+1)D backbone also achieves the best result on UCF101 and HMDB51. It indicates that FAME helps MoCo learn the scene-debiased and motion-aware representations on the Kinetics-400 dataset, which generalize well to the downstream dataset. Remarkably, FAME brings 1.9% and 2.8% performance gain on UCF101 and HMDB51 against the MoCo baseline. In comparison to other state-of-the-art methods, although SRTC (Zhang et al. 2021) introduces two additional sub-loss terms to regularize the self-supervised pretraining, our simple formulation outperforms SRTC by 2.8% and 2.3% with the same backbone R(2+1)D. Notably, we share similar motivation with BE (Wang et al. 2021b), both hoping to alleviate the background bias problem by disturbing the background. BE directly adds a static frame to every other frame and regards this distracting video as the positive pair to the original video. This coarse disturbance ruins the foreground region, and our experiments testify that it does hurt the temporal modeling and motion understanding. Using the

Method	Backbone	R@k				
		R@1	R@5	R@10	R@20	R@50
SpeedNet (Benaim et al. 2020)	S3D-G	13.0	28.1	37.5	49.5	65.0
MLRep (Qian et al. 2021)	R3D-18	41.5	60.0	71.2	80.1	-
ASCNet (Huang et al. 2021a)	R3D-18	58.9	76.3	82.2	87.5	93.4
FAME (ours)	R(2+1)D	62.3	75.1	80.9	86.9	93.0

Table 2: Comparison with the existing self-supervised video representation learning methods for video retrieval. All methods are pretrained on Kinetics-400. We report the Top-k recall R@k when k=1, 5, 10, 20, 50 on UCF101.

β	UCF101	HMDB51
1.0 (baseline)	75.8	45.5
0.7	80.3	49.6
0.5	81.2	**52.6**
0.3	**82.0**	51.6

Table 3: Top-1 accuracy with respect to β on UCF101 and HMDB51. $\beta = 0.3$ is optimal for UCF101 and $\beta = 0.5$ achieves best on HMDB51.

Background	UCF101	HMDB51
none	75.8	45.5
intra-video	77.4(1.6↑)	47.6(2.1↑)
inter-video	81.2(5.4↑)	52.6(7.1↑)

Table 4: Top-1 accuracy on UCF101 and HMDB51 in terms of intra-/inter-video background. Using the inter-video background increases the accuracy more greatly than using the intra-video background.

same backbone I3D, FAME outperforms BE by 1.8% and 5.7% on UCF101 and HMDB51, respectively. It proves that our model can better mitigate the static background bias by further separating foreground and background.

Video Retrieval. We report the performance comparison for video retrieval in Table 2. Our method achieves significant performance gain on R@1. Remarkably, though ASC-Net (Huang et al. 2021a) devises two particular tasks to learn appearance and speed consistency, we still reach higher Top-1 retrieval accuracy. It is because our motion-aware representations can precisely retrieve the action with the same semantics. Ours is slightly lower than ASCNet in R@5 to R@50 since FAME almost abandons background cues, while ASCNet may take trace of background shortcuts to retrieve samples of the same category when k is large.

4.4 Ablation Study

In this section, we conduct thorough ablation studies to analyze how FAME improves self-supervised video representation learning. We choose split 1 of UCF101 as the pretrain dataset and I3D as the backbone for computational efficiency. All the Top-1 accuracy in the ablation study is measured under the protocol of finetune.

Importance of the area ratio of the foreground region. In this section, we inspect how the area of the foreground region contributes to the representation quality. We ablate β, the portion of the foreground, in the range of $\{1, 0.7, 0.5, 0.3\}$. Note that $\beta = 1$ reverts to the baseline method without applying FAME. We report the performance in Table 3. It can be observed that the results of $\beta = 0.3$ and 0.5 vastly outperform baseline by $\sim 6\%$ on both UCF101 and HMDB51. The improvement of $\beta = 0.7$ is also considerable, though slightly inferior to the smaller value of β due to insufficient background replacement. This phenomenon shows that our method is insensitive to the hyper-parameter

β, and the harder contrastive task formulated by FAME is more conducive to the representation quality.

Impact of background source. Besides the foreground ratio, we also wonder how the source of background affects the representation ability to capture the motion. Specifically, we aim to explore whether the performance would change dramatically using the background in the same video instead of other videos. We perform an additional experiment where we merge the foreground of one video with the background sampled at different timestamps of the video itself. As shown in Table 4, we find that using the background from intra-video boosts the baseline with 1.6% and 2.1% improvement on UCF101 and HMDB51 and the introduction of other videos' backgrounds brings further improvement, i.e., 5.4% and 7.1% gain on UCF101 and HMDB51. In general, the intra-video background is almost the same as the original one, while the inter-video background is quite distinct. Thus, it demonstrates that the modification from the intra-video is not adequate to mitigate background bias while replacing the background with diverse scenes better strengthens motion pattern learning.

Stronger background debiasing. To explore whether FAME is sufficiently strong to reduce the background bias in the contrastive learning, we design a stronger contrastive objective. That is, we apply FAME on both branches of MoCo and neither of the two processed video clips contains initial background information. We report the results in Table 5. The slight difference in performance between those two settings proves that our default setting is strong enough for the model to learn the scene-debiased representations.

Variants of Foreground-background Separation. In order to verify that emphasizing moving foreground advances the motion understanding, we devise three variants of foreground mask: (i) Gauss: we adopt a 2D Gaussian kernel matrix as the foreground mask. It derives from the assumption

	UCF101		HMDB51	
β	single	both	single	both
0.7	80.3	79.6	49.6	50.8
0.5	81.2	81.2	52.6	51.4
0.3	82.0	81.1	51.6	53.1

Table 5: Top-1 accuracy on UCF101 and HMDB51. We denote the operating FAME on single branch (default setting) as *single* and the operating FAME on both branches as *both*. Under various β, the corresponding value of single and both is approximately the same.

Method	UCF101	HMDB51
baseline	75.8	45.5
Gauss	77.9	46.4
Seed	80.4	51.3
Grid	81.5	51.5
FAME	81.2	52.6
Grid†	86.5	58.7
FAME†	88.6	61.1

Table 6: Top-1 accuracy of various foreground-background separation methods on UCF101 and HMDB51. † indicates the pretrain dataset is Kinetics-400. All variants improve the baseline significantly and FAME performs best.
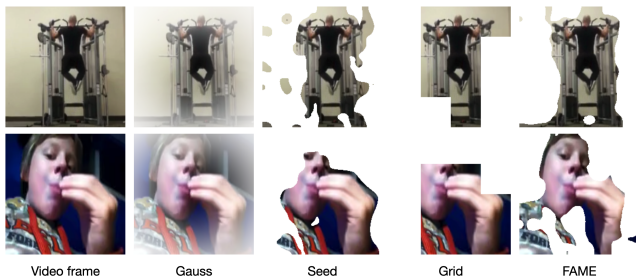

Figure 3: The illustration about FAME and three variants of foreground-background separation.

that videos are shot in the object-centric form. (ii) Seed: we just take the seed region S to characterize the foreground. (iii) Grid: we separate foreground and background via the grid. In practice, the video is split into 4×4 grids spatially. We count the sum of S in each grid and take the greatest eight grids as the foreground area. A brief illustration is displayed in Figure 3.

We compare FAME with these three variants in Table 6. First, we note that all variants improve the baseline by a large margin, showing the effect of FAME. Furthermore, refining the foreground mask from Gauss, Seed, Grid to FAME continually increases the action recognition performance. Interestingly, we notice that Grid outperforms FAME slightly on UCF101. We conjecture that it is because both the pretrain dataset and downstream dataset are UCF101. Thus, background bias can be leveraged as a shortcut for action recognition. To delve into this phenomenon, we carry out an extra experiment on another pretrain dataset Kinetics-400. Top-1
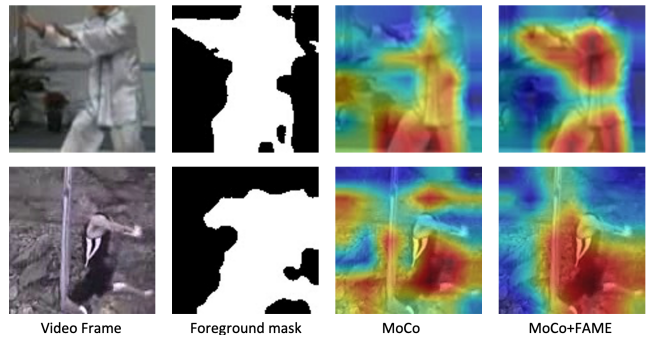

Figure 4: Class activation maps (CAM) visualization. Red areas indicate the important areas for the model to predict the action class. Comparing to MoCo, MoCo+FAME resists the impact of background and highlights the motion areas.

accuracy of Grid variant is over 2% lower than FAME on both UCF101 and HMDB51. It indicates that a meticulous segmentation mask instead of a rough grid box is more effective in facilitating generalization ability.

4.5 Visualization Analysis
To better demonstrate the effectiveness of FAME, we provide the CAM (Zhou et al. 2016) visualization in Figure 4. We train a linear classifier with the pretrained model similar to the linear probe and omit the last global average pooling layer to generate activation maps. With that, we can spot the contribution of each area and find crucial regions for discriminating the action class. We find that when integrated with FAME, MoCo can focus on moving foreground area rather than background context. For example, in the first row of Figure 4, MoCo+FAME precisely captures the moving upper and lower body when the man is practicing TaiChi, while the MoCo baseline displays a dispersed highlight map and fails to attend to the motion area. In addition, we illustrate that the CAM activation map can almost overlap with the foreground mask generated by FAME. It testifies that our method enables the model to perceive the motion patterns and hinder the background bias.

5 Conclusion
In this work, we propose a new Foreground-background Merging (FAME) method to alleviate the background bias in self-supervised video representation learning. Via Foreground-background Merging, we augment the original video by separating the foreground and background regions and fusing the original foreground with other videos' backgrounds. Then, the backbone model is trained to learn semantically consistent representation between the original video and the fused video. In this way, the model can learn the scene-debiased and motion-aware representations of videos. Experimental results on a bunch of downstream tasks manifest the effectiveness of our method.

References

Abu-El-Haija, S.; Kothari, N.; Lee, J.; Natsev, P.; Toderici, G.; Varadarajan, B.; and Vijayanarasimhan, S. 2016. Youtube-8m: A large-scale video classification benchmark. *arXiv preprint arXiv:1609.08675*.

Asano, Y. M.; Rupprecht, C.; and Vedaldi, A. 2019. Self-labelling via simultaneous clustering and representation learning. *arXiv preprint arXiv:1911.05371*.

Benaim, S.; Ephrat, A.; Lang, O.; Mosseri, I.; Freeman, W. T.; Rubinstein, M.; Irani, M.; and Dekel, T. 2020. Speed-net: Learning the speediness in videos. In *Proceedings of the IEEE/CVF Conference on Computer Vision and Pattern Recognition*, 9922–9931.

Carreira, J.; and Zisserman, A. 2017. Quo vadis, action recognition? a new model and the kinetics dataset. In *Proceedings of the IEEE/CVF Conference on Computer Vision and Pattern Recognition*, 6299–6308.

Chen, P.; Huang, D.; He, D.; Long, X.; Zeng, R.; Wen, S.; Tan, M.; and Gan, C. 2021. Rspnet: Relative speed perception for unsupervised video representation learning. In *Proceedings of the AAAI Conference on Artificial Intelligence*, volume 1.

Chen, T.; Kornblith, S.; Norouzi, M.; and Hinton, G. 2020a. A simple framework for contrastive learning of visual representations. In *International conference on machine learning*, 1597–1607. PMLR.

Chen, X.; Fan, H.; Girshick, R.; and He, K. 2020b. Improved baselines with momentum contrastive learning. *arXiv preprint arXiv:2003.04297*.

Choi, J.; Gao, C.; Messou, C. E. J.; and Huang, J.-B. 2019. Why Can't I Dance in the Mall? Learning to Mitigate Scene Bias in Action Recognition. In *NeurIPS*.

Feichtenhofer, C.; Fan, H.; Malik, J.; and He, K. 2019. Slow-fast networks for video recognition. In *Proceedings of the IEEE international conference on computer vision*, 6202–6211.

Feichtenhofer, C.; Fan, H.; Xiong, B.; Girshick, R.; and He, K. 2021. A Large-Scale Study on Unsupervised Spatiotemporal Representation Learning. In *Proceedings of the IEEE/CVF Conference on Computer Vision and Pattern Recognition*, 3299–3309.

Gordon, D.; Ehsani, K.; Fox, D.; and Farhadi, A. 2020. Watching the world go by: Representation learning from unlabeled videos. *arXiv preprint arXiv:2003.07990*.

Goyal, R.; Ebrahimi Kahou, S.; Michalski, V.; Materzynska, J.; Westphal, S.; Kim, H.; Haenel, V.; Fruend, I.; Yianilos, P.; Mueller-Freitag, M.; et al. 2017. The" something something" video database for learning and evaluating visual common sense. In *Proceedings of the IEEE international conference on computer vision*, 5842–5850.

Grill, J.-B.; Strub, F.; Altché, F.; Tallec, C.; Richemond, P. H.; Buchatskaya, E.; Doersch, C.; Pires, B. A.; Guo, Z. D.; Azar, M. G.; et al. 2020. Bootstrap your own latent: A new approach to self-supervised learning. *arXiv preprint arXiv:2006.07733*.

Gutmann, M.; and Hyvärinen, A. 2010. Noise-contrastive estimation: A new estimation principle for unnormalized statistical models. In *Proceedings of the Thirteenth International Conference on Artificial Intelligence and Statistics*, 297–304. JMLR Workshop and Conference Proceedings.

Han, T.; Xie, W.; and Zisserman, A. 2019. Video representation learning by dense predictive coding. In *Proceedings of the IEEE international conference on computer vision Workshops*, 0–0.

Han, T.; Xie, W.; and Zisserman, A. 2020a. Memory-augmented dense predictive coding for video representation learning. In *Proceedings of the European conference on computer vision*, 312–329. Springer.

Han, T.; Xie, W.; and Zisserman, A. 2020b. Self-supervised co-training for video representation learning. *arXiv preprint arXiv:2010.09709*.

He, K.; Fan, H.; Wu, Y.; Xie, S.; and Girshick, R. 2020. Momentum contrast for unsupervised visual representation learning. In *Proceedings of the IEEE/CVF Conference on Computer Vision and Pattern Recognition*, 9729–9738.

He, Y.; Shirakabe, S.; Satoh, Y.; and Kataoka, H. 2016. Human action recognition without human. In *European Conference on Computer Vision*, 11–17. Springer.

Huang, D.; Wu, W.; Hu, W.; Liu, X.; He, D.; Wu, Z.; Wu, X.; Tan, M.; and Ding, E. 2021a. ASCNet: Self-supervised Video Representation Learning with Appearance-Speed Consistency. *arXiv preprint arXiv:2106.02342*.

Huang, L.; Liu, Y.; Wang, B.; Pan, P.; Xu, Y.; and Jin, R. 2021b. Self-supervised Video Representation Learning by Context and Motion Decoupling. In *Proceedings of the IEEE/CVF Conference on Computer Vision and Pattern Recognition*, 13886–13895.

Jenni, S.; Meishvili, G.; and Favaro, P. 2020. Video representation learning by recognizing temporal transformations. In *Proceedings of the European conference on computer vision*, 425–442. Springer.

Jing, L.; Yang, X.; Liu, J.; and Tian, Y. 2018. Self-supervised spatiotemporal feature learning via video rotation prediction. *arXiv preprint arXiv:1811.11387*.

Kim, D.; Cho, D.; and Kweon, I. S. 2019. Self-supervised video representation learning with space-time cubic puzzles. In *Proceedings of the AAAI Conference on Artificial Intelligence*, volume 33, 8545–8552.

Kong, Q.; Wei, W.; Deng, Z.; Yoshinaga, T.; and Murakami, T. 2020. Cycle-contrast for self-supervised video representation learning. *arXiv preprint arXiv:2010.14810*.

Kuehne, H.; Jhuang, H.; Garrote, E.; Poggio, T.; and Serre, T. 2011. HMDB: a large video database for human motion recognition. In *2011 International conference on computer vision*, 2556–2563. IEEE.

Lee, H.-Y.; Huang, J.-B.; Singh, M.; and Yang, M.-H. 2017. Unsupervised representation learning by sorting sequences. In *Proceedings of the IEEE international conference on computer vision*, 667–676.

Li, Y.; Li, Y.; and Vasconcelos, N. 2018. Resound: Towards action recognition without representation bias. In *Proceedings of the European conference on computer vision*, 513–528.

Luo, D.; Liu, C.; Zhou, Y.; Yang, D.; Ma, C.; Ye, Q.; and Wang, W. 2020. Video cloze procedure for self-supervised spatio-temporal learning. In *Proceedings of the AAAI Conference on Artificial Intelligence*, volume 34, 11701–11708.

Misra, I.; Zitnick, C. L.; and Hebert, M. 2016. Shuffle and learn: unsupervised learning using temporal order verification. In *European Conference on Computer Vision*, 527–544. Springer.

Oord, A. v. d.; Li, Y.; and Vinyals, O. 2018. Representation learning with contrastive predictive coding. *arXiv preprint arXiv:1807.03748*.

Pan, T.; Song, Y.; Yang, T.; Jiang, W.; and Liu, W. 2021. Videomoco: Contrastive video representation learning with temporally adversarial examples. In *Proceedings of the IEEE/CVF Conference on Computer Vision and Pattern Recognition*, 11205–11214.

Qian, R.; Li, Y.; Liu, H.; See, J.; Ding, S.; Liu, X.; Li, D.; and Lin, W. 2021. Enhancing Self-supervised Video Representation Learning via Multi-level Feature Optimization. *arXiv preprint arXiv:2108.02183*.

Qian, R.; Meng, T.; Gong, B.; Yang, M.-H.; Wang, H.; Belongie, S.; and Cui, Y. 2020. Spatiotemporal contrastive video representation learning. *arXiv preprint arXiv:2008.03800*.

Soomro, K.; Zamir, A. R.; and Shah, M. 2012. UCF101: A dataset of 101 human actions classes from videos in the wild. *arXiv preprint arXiv:1212.0402*.

Stretcu, O.; and Leordeanu, M. 2015. Multiple Frames Matching for Object Discovery in Video. In *BMVC*, volume 1, 3.

Sun, C.; Baradel, F.; Murphy, K.; and Schmid, C. 2019. Learning video representations using contrastive bidirectional transformer. *arXiv preprint arXiv:1906.05743*.

Tao, L.; Wang, X.; and Yamasaki, T. 2020. Self-supervised video representation learning using inter-intra contrastive framework. In *ACM MM*, 2193–2201.

Tian, Y.; Krishnan, D.; and Isola, P. 2019. Contrastive multiview coding. *arXiv preprint arXiv:1906.05849*.

Tran, D.; Wang, H.; Torresani, L.; Ray, J.; LeCun, Y.; and Paluri, M. 2018. A closer look at spatiotemporal convolutions for action recognition. In *Proceedings of the IEEE conference on Computer Vision and Pattern Recognition*, 6450–6459.

Vondrick, C.; Shrivastava, A.; Fathi, A.; Guadarrama, S.; and Murphy, K. 2018. Tracking emerges by colorizing videos. In *Proceedings of the European conference on computer vision*, 391–408.

Wang, J.; Gao, Y.; Li, K.; Jiang, X.; Guo, X.; Ji, R.; and Sun, X. 2021a. Enhancing unsupervised video representation learning by decoupling the scene and the motion. In *Proceedings of the AAAI Conference on Artificial Intelligence*.

Wang, J.; Gao, Y.; Li, K.; Lin, Y.; Ma, A. J.; Cheng, H.; Peng, P.; Huang, F.; Ji, R.; and Sun, X. 2021b. Removing the Background by Adding the Background: Towards Background Robust Self-supervised Video Representation Learning. In *Proceedings of the IEEE/CVF Conference on Computer Vision and Pattern Recognition*, 11804–11813.

Wang, J.; Jiao, J.; Bao, L.; He, S.; Liu, Y.; and Liu, W. 2019. Self-supervised spatio-temporal representation learning for videos by predicting motion and appearance statistics. In *Proceedings of the IEEE/CVF Conference on Computer Vision and Pattern Recognition*, 4006–4015.

Wang, J.; Jiao, J.; and Liu, Y.-H. 2020. Self-supervised video representation learning by pace prediction. In *Proceedings of the European conference on computer vision*.

Wang, L.; Xiong, Y.; Wang, Z.; Qiao, Y.; Lin, D.; Tang, X.; and Van Gool, L. 2016. Temporal segment networks: Towards good practices for deep action recognition. In *European conference on computer vision*, 20–36. Springer.

Wu, Z.; Xiong, Y.; Yu, S. X.; and Lin, D. 2018. Unsupervised feature learning via non-parametric instance discrimination. In *Proceedings of the IEEE conference on computer vision and pattern recognition*, 3733–3742.

Xiao, F.; Tighe, J.; and Modolo, D. 2021. MoDist: Motion Distillation for Self-supervised Video Representation Learning. *arXiv preprint arXiv:2106.09703*.

Xu, D.; Xiao, J.; Zhao, Z.; Shao, J.; Xie, D.; and Zhuang, Y. 2019. Self-supervised spatiotemporal learning via video clip order prediction. In *Proceedings of the IEEE/CVF Conference on Computer Vision and Pattern Recognition*, 10334–10343.

Yao, Y.; Liu, C.; Luo, D.; Zhou, Y.; and Ye, Q. 2020. Video playback rate perception for self-supervised spatio-temporal representation learning. In *Proceedings of the IEEE/CVF Conference on Computer Vision and Pattern Recognition*, 6548–6557.

Zhang, L.; She, Q.; Shen, Z.; and Wang, C. 2021. How Incomplete is Contrastive Learning? An Inter-intra Variant Dual Representation Method for Self-supervised Video Recognition. *arXiv preprint arXiv:2107.01194*.

Zhou, B.; Khosla, A.; Lapedriza, A.; Oliva, A.; and Torralba, A. 2016. Learning deep features for discriminative localization. In *Proceedings of the IEEE international conference on computer vision*, 2921–2929.